



Published in final edited form as:

J Med Chem. 2012 May 10; 55(9): 4220–4230. doi:10.1021/jm201699w.

Non-nucleoside Inhibitors of the Measles Virus RNA-dependent RNA Polymerase: Synthesis, Structure-Activity Relationships and Pharmacokinetics

J. Maina Ndungu¹, Stefanie A. Krumm², Dan Yan², Richard F. Arrendale¹, G. Prabhakar Reddy¹, Taylor Evers¹, Randy Howard¹, Michael G. Natchus¹, Manohar T. Saindane¹, Dennis C. Liotta^{1,3}, Richard K. Plempner^{2,4}, James P. Snyder^{1,3}, and Aiming Sun^{*,1}

¹Emory Institute for Drug Discovery, Emory University, 1515 Dickey Dr. Atlanta, GA, 30322

²Department of Pediatrics, Emory University School of Medicine, 2015 Uppergate Dr. Atlanta, GA, 30322

³Department of Chemistry, Emory University, 1515 Dickey Dr. Atlanta, GA, 30322

⁴Children's Healthcare of Atlanta, 2015 Uppergate Dr. Atlanta, Georgia, 30322

Abstract

The measles virus (MeV), a member of the paramyxovirus family, is an important cause of pediatric morbidity and mortality worldwide. In an effort to provide therapeutic treatments for improved measles management, we previously identified a small, non-nucleoside organic inhibitor of the viral RNA-dependent RNA polymerase (RdRp) by means of high-throughput screening (HTS). Subsequent structure-activity relationship (SAR) studies around the corresponding pyrazole carboxamide scaffold led to the discovery of **2** (AS-136a), a first generation lead with low nanomolar potency against life MeV and attractive physical properties suitable for development. However, its poor water solubility and low oral bioavailability (F) in the rat suggested that the lead could benefit from further SAR studies to improve the biophysical characteristics of the compound. Optimization of *in vitro* potency and aqueous solubility led to the discovery of **2o** (ERDRP-00519), a potent inhibitor of MeV (EC₅₀ = 60 nM) with aqueous solubility of approximately 60 µg/ml. The agent shows a 10-fold exposure (AUC/Cmax) increase in the rat model relative to **2**, displays near dose proportionality in the range of 10 mg/kg to 50 mg/kg, and exhibits good oral bioavailability (F = 39%) in the rat. The significant solubility increase appears linked to the improved oral bioavailability.

Keywords

measles virus; RNA-dependent RNA polymerase activity inhibitor; AS-136a; ERDRP-00519; pharmacokinetics

*Corresponding author: Phone: 404-712-8680; asun2@emory.edu.

Supporting Information Available. Experimental details for the preparation of compounds **7a-c**, **2b**, **2c**, **2d**, **2e**, **2f**, **2g**, **2h**, **2i**, **2j**, **2o**, **2p**, **2q**, **3b**, **17-19**, **3f**, and **3g**; Supplementary Scheme S1 (Synthetic Scheme for the synthesis of morpholinyl analog **2o**); Supplementary Figure S1 (Mean plasma concentration following i.v. and p.o. dosing of **2o** in Sprague-Dawley rat); Supplementary Table S1 (Summary of **2o** Pharmacokinetic properties). This material is available free of charge via the Internet at <http://pubs.acs.org>.

INTRODUCTION

The paramyxoviruses family comprised non-segmented, negative strand RNA viruses that are primarily responsible for acute respiratory diseases. The family includes major human and animal pathogens such as measles virus (MeV), human parainfluenza virus (HPIV), mumps virus, respiratory syncytial virus (RSV) and the Newcastle disease virus. Despite the existence of an effective vaccine protecting against MeV infection, we have witnessed in the recent past an increasing number of cases particularly in the developed world.^{1,2} For example, in the United States from January 1 through May 21 of 2011, 118 cases were reported across 23 states according to the CDC. Recently, in Ashland, Oregon, 25-30% of children entering kindergarten were unvaccinated.³ This has been attributed to elected exemption from vaccination on the basis of philosophical or religious beliefs. Vaccination rates in Europe in recent years have never fully recovered from a discredited 1998 British study linking the vaccine for measles, mumps and rubella to autism. At that time, parents, particularly in the U.K. abandoned the vaccine followed by precipitous drops in vaccination rates. For 2011, the World Health Organization reported 4,937 cases of measles between January and March in France alone, compared with 5,090 cases during all of 2010. The World Health Organization reports that as of October, there have been 26,000 measles cases, and nine deaths, in Europe since the start of 2011, rendering it the worst year for MeV activity in the Western World since 1996.⁴

Measles is not currently treatable by drug therapy. Ribavirin, a nucleoside based anti-viral agent, is the only small molecule drug approved for paramyxoviruses (RSV) therapy.^{5, 6} However, efficacy is limited. To improve case management of severe measles and achieve rapid control of outbreaks through post-exposure prophylaxis, the development of an effective anti-measles drug is highly desirable.⁷ We previously reported the discovery of an MeV inhibitor targeting the viral RNA dependent RNA polymerase (RdRp) complex by means of a cell-based high-throughput screening (HTS).^{8,9} Iterative optimization of a corresponding series of pyrazole carboxamides, exemplified by hit **1** (16677), led to the first-generation lead molecule **2** (AS-136a) (Figure 1).^{10,11} The latter piperidine derivative exhibits superior *in vitro* cellular potency against MeV with nanomolar EC₅₀ concentrations. It was also subjected to a number of *in vitro* toxicity and metabolism assays. There, the compound was found to be non-mutagenic in a non-GLP *in vitro* bacterial reverse mutation (Ames) assay, and it did not block hERG channels at a concentration of 10 μ M or below. Compound **2** shows moderate metabolic stability in mouse and human S9 fractions after one-hour incubation with 79% and 69% parent remaining, respectively. However, poor solubility and low rat plasma concentrations of **2** might hamper its *in vivo* efficacy. In an effort to improve pharmacological properties of **2**, in particular water solubility, we initiated a structure activity relationship (SAR) study to identify a suitable solubilizing group. Earlier efforts had shown that the piperidine ring is amenable to chemical manipulation without adversely affecting activity. However, any changes to the central ring or the pyrazole group of **2** are detrimental to activity.¹¹ Consequently, the present study focuses on appending a solubilizing group to the piperidine ring or replacing it with either a substituted phenyl or an alicyclic group. This led to the identification of compound **2o** (ERDRP-00519, Figure 1), which has significantly improved water solubility, while retaining high antiviral potency. The agent shows a 10-fold exposure (AUC/C_{max}) increase in rat relative to **2** and displays near dose proportionality in the range of 10 mg/kg to 50 mg/kg. The significant solubility increase appears to contribute to the improvement in oral bioavailability. We describe herein the synthesis and a structure-activity relationship (SAR) strategy that led to the discovery of **2o** as well as the pharmacokinetic comparison of first and second-generation lead candidates.

CHEMISTRY

Synthesis of Substituted Piperidine Analogs

Our previous work showed that introduction of a piperidine moiety resulted in compounds that were about 10 times more active than the corresponding pyrrolidine analogs.¹⁰ Accordingly, linkers were installed at the 2-, 3- and 4-positions of the pyrrolidine ring to explore which position could best accommodate hydrophilic substituents while maintaining potency. Reaction of different amino alcohols (**4a-c**) with 4-nitrobenzene sulfonyl chloride (**5**) followed by formation of methoxymethyl (MOM) ethers and reduction of the nitro group afforded anilines **7a-c**. Coupling of acid chloride **8**, derived from 3-trifluoromethyl pyrazole using the method of Lahm,¹² with anilines **7a-c** provided analogs **1a-c** (Scheme 1). With preliminary data showing the 2-position of the piperidine to yield more active compounds compared to the 3- or 4-position (Table 1), additional analogs of the previously reported 2-piperidinemethanol compound **2a**¹³ were prepared by a sequence similar to that depicted in Scheme 1.

Further analogs were prepared by PCC oxidation of **6a** to obtain aldehyde **14**, which was subjected to reductive amination with morpholine followed by the procedures illustrated in Schemes 2 to ultimately give analog **2b**. Tosylation of **6a**, reduction of the nitro group, coupling with acid chloride **8** and displacement of the tosylate with an azide furnished **2c**. Reduction of the azide, dimethylation of the resultant amine or acylation resulted in compounds **2d-f**. Further extension of the side chain including both saturated and unsaturated derivatives could be achieved from aldehyde **14**. Horner-Wadsworth-Emmons olefination of **14** gave **12**. Union of **12** with acid chloride **8** afforded analog **2g**, which was then reduced with DIBAL-H to obtain analog **2h**. Hydrogenation of **2g** delivered the saturated analog **2i**, which was converted to **2j** by treatment with DIBAL-H (Scheme 2).

Preparation of two-carbon side chain analogs was accomplished by utilizing 2-(2-piperidinyl) ethanol **9**. Direct coupling of the latter with *p*-nitro-benzenesulfonyl chloride **5** gave low yields of the desired product due to further coupling of the product with the sulfonyl chloride. To circumvent this shortcoming, the NH- and OH- groups of **9** were protected using benzyl chloroformate¹⁴ and *t*-butyldimethylsilyl chloride (TBSCl), respectively. De-protection of the amine, coupling with **5** and reduction of the nitro group afforded aniline **11**. Coupling of **11** with acid chloride **8** followed by cleavage of the silyl group furnished alcohol **2k** which, when subjected to Swern oxidation and reductive amination with morpholine, gave **2n** (Scheme 3). Chiral pure enantiomer **2o** was then prepared similar to **2n** starting from (*S*)-2-piperidine ethanol.

We hypothesized that attaching an ethylene glycol moiety would give compounds with better aqueous solubility. Due to the instability of **6a** under basic conditions, the synthesis of **2p** was initiated by addition of a rhodium carbenoid across the hydroxylic bond^{15,16} to form an ether bond. Thus, decomposition of ethyl diazoacetate in the presence of Rh₂OAc₄ generated a carbenoid that inserted into the OH bond to give **13**. Reduction of the nitro group of **13** followed by coupling with **8** afforded analog **2p**, which on hydrolysis of the ester and BOP/NaBH₄¹⁷ mediated reduction of the resultant carboxylic acid, provided **2q** (Scheme 4).

Synthesis of the Phenyl Series

Replacement of the piperidine ring with phenyl or substituted phenyl *via* the general route shown in Scheme 5 was also explored. Unsubstituted phenyl analog **3a** was found to be as active as lead compound **2** triggering an SAR study of the series (Table 2). Coupling of 2-methoxythiophenol **16a** with 1-fluoro-4-nitrobenzene¹⁸ followed by oxidation of sulfur

using MCPBA gave corresponding sulfone, which went through reduction of the nitro group and followed by coupling with acid chloride **8** furnished analog **3b**. Demethylation of **3b** with BBr₃ afforded phenol analog **3c**, which on acylation gave analog **3d**. Similarly, coupling of 2-bromothiophenol **16b** with 1-fluoro-4-nitrobenzene obtained **17**. To make additional analogs of the phenyl series, we envisioned utilizing bromide **17** to append substituents. However, attempts to lithiate bromide **17** using *n*-BuLi or *t*-BuLi were unfruitful resulting in decomposition of the bromide. Stille coupling offered an alternative. When **17** was treated with tributyl(vinyl)tin in the presence of Pd(PPh₃)₄, the desired coupling product **18** was obtained in 80% yield. Reduction of the nitro group followed by coupling with acid chloride **8** afforded analog **3e** (Scheme 5 and Table 2). Subjecting olefin **18** to osmium tetroxide-mediated oxidative cleavage of the double bond gave aldehyde **19**, a compound utilized in the synthesis of additional analogs. Reduction of the aldehyde, SnCl₂ reduction of the nitro group and protection of the alcohol as a silyl ether gave aniline **20**. Coupling of **20** with acid chloride **8** followed by cleavage of the silyl group furnished analog **3f**. Aldehyde **19** was also used for the synthesis of morpholine **3g** by means of reductive-amination, followed by reduction of the nitro group and coupling with acid chloride **8** (Scheme 5).

Single Dose Antiviral Activity of Analogs of **2**

In order to better understand the potency profile of compound **2** analogs, the most active analogs were subjected to a measles virus yield assay at a single concentration of 1.0 μM to generate data points for comparison with **2**.

RESULTS AND DISCUSSION

The SAR data are summarized in Tables 1 and 2 for the piperidine and phenyl series, respectively. From previous experience, we have learned the necessity of preserving the structure of the phenyl, amide and fluorinated pyrazole units of the molecule in order to maintain anti-viral potency. Modification of either the 3-trifluoromethyl-pyrazole or the central phenyl ring in most cases leads to significant loss of activity.^{10,11} All analogs listed in Tables 1 and 2 incorporate only variations on the left side of lead molecule **1**. The MOM ether analogs (**1a-c**) demonstrate a trend whereby substitution at C-2 of the piperidine is favored. The 2-piperidine **1a** is 2-fold more potent than the corresponding 3-piperidine, while the 4-substituted derivatives reduce activity by almost 10-fold (**1a**, **1b** and **1c**, Table 1). For compounds with a hydroxyl group, elongation of the pendant chain from one carbon to two does not adversely affect potency as exemplified by compounds **2a** and **2k**.

Further extension to three carbons leads to a decrease in activity by 3-fold (**2j**, Table 1). Introduction of basic amines led to significant reduction or complete loss of activity (**2d** and **2f**, EC₅₀ = 55.0 and >150 μM, respectively). Replacement of the amino groups with a less basic morpholine (**2b** and **2n**) restored good potency. Esters **2g** and **2i** were found to be 2-fold less active by comparison with the corresponding alcohols (**2h** and **2j**, Table 1). There is a clear superiority of *S*-chirality over *R*- as demonstrated by the 3-fold loss of activity for **2l** compared to **2m**. For the phenyl series, analog **3a** is as active as the lead compound in reducing virus-induced cytopathicity, and its activity is comparable to that of methoxy **3b** and alcohol **3f** (Table 3). However, the morpholine analog **3g** loses activity completely, which stands in significant contrast to alterations in the piperidine series (**2b** and **2n**). The previous SAR and that derived from the current three series of MeV-RdRp inhibitors suggests a highly hydrophobic environment on the target protein housing the left part of the molecules, strongly disfavoring hydrogen bonding. To explore whether poor aqueous solubility contributes to the low oral bioavailability that was observed with the existing lead **2**, we measured the aqueous solubility for some of the more potent derivatives *via*

nephelometry (buffer, pH = 7.4, Table 3). **2** and phenyl analog **3a** show equally poor solubility with values at 15 $\mu\text{g/ml}$ and 22 $\mu\text{g/ml}$, respectively. The alcohol analogs **2a** and **2k** both deliver improved solubility as expected with measured values at 61 and 62 $\mu\text{g/ml}$, respectively. Importantly, the morpholine analog **2n** also furnishes similar solubility compared with the corresponding free alcohol derivative **2k**. Compounds with moderate solubility (~ 60 $\mu\text{g/ml}$) and good potency (< 3.0 μM) in the CPE assay were advanced to assessment of virus yield reduction. The primary alcohol derivative **2k** (EC_{50} 2.7 μM , CPE assay; solubility 62 $\mu\text{g/ml}$) delivers an EC_{50} of 100 nM in this assay (**2k**; Table 3). Optically pure analogs of compound **2k**, **2l** and **2m**, both delivered slightly decreased potency (EC_{50} 8.3 and 3.1 μM , respectively, CPE assay). Replacement of the hydroxyl group with morpholine led to racemate **2n** with an EC_{50} of 4.6 μM , while the corresponding optically pure analog **2o** provided an EC_{50} of 2.5 μM in the CPE assay, 60 nM in the virus yield reduction assay and solubility around 60 $\mu\text{g/ml}$ (**2o**; Table 3).

Considering the advanced potencies of **2k** and **2o** in the virus yield reduction assay (EC_{50} = 100 and 60 nM, respectively), we selected these two compounds for comparison with **2** in a pharmacokinetic (PK) study in Sprague-Dawley rats.

PHARMACOKINETIC PROFILES

Figure 3 shows oral pharmacokinetic parameters of compounds **2k** and **2o** in comparison with the first generation lead **2**; a summary of the numerical PK analysis is provided in Table 4. Compound **2o** shows a 10-fold exposure (with respect to both AUC and C_{max}) increase in the rat model relative to **2** and displays good dose proportionality in the range of 10 mg/kg to 50 mg/kg. In contrast, the primary alcohol analog **2k** reveals a good C_{max} and AUC at 50 mg/kg dosing, but it generates poor plasma concentrations in rat and non-proportionality possibly due to high first-pass metabolism of the primary alcohol. On the basis of its high *in vitro* potency, good solubility and pharmacokinetic profile, the oral bioavailability of compound **2o** was assessed. The compound was dosed at 2 mg/kg i.v. and 10 mg/kg p.o. in rat and exhibits good oral bioavailability ($F = 39\%$) (Figure S1 and Table S1). In the Caco-2 bi-directional permeability assay, both **2** and **2o** showed high permeability with an efflux ratio of 1.1 and 2.6, respectively, which indicates that they are probably not a substrate for p-glycoprotein in humans. (Figure S2)^{19, 20} However, compound **2o** proved to be less stable in human liver S9 fractions after one hour incubation. Only 24% of the parent remains as compared with 69% for compound **2**.

Mechanism of Action of **2o**

We previously demonstrated that compound **2** blocks MeV RdRp activity by targeting the viral polymerase (L) protein.¹¹ To test whether this mechanism of activity likewise extends to lead molecule **2o**, a plasmid-based mini-replicon assay²¹ was employed to assess RdRp activity in the presence of **2o** and **2**, respectively. BSR-T7/5 cells were transfected with plasmid DNA encoding MeV-L, N, P and the firefly luciferase mini-genome reporter construct, and the cell were incubated in the presence of different inhibitor concentrations or vehicle for control. Relative luciferase activities in cell lysates were assessed 36 hours post-transfection and dose-response inhibition curves generated. For both compounds, we observed a dose-dependent inhibition of viral RdRp activity with virtually identical potency (Figure 4), supporting comparable mechanism of antiviral activity.

SUMMARY

Modification and replacement of the piperidine moiety in the first-generation lead **2**, derived from our MeV-RdRp inhibitor program has been investigated. An SAR study revealed that hydrophilicity in this molecular sector strongly influences antiviral activity. We identified

compounds incorporating hydroxyl (**2k**) and morpholinyl (**2o**) moieties that furnish potencies within a 10-fold range of **2**, but with much improved aqueous solubility and oral bioavailability. In the series that replaces piperidine with the phenyl group, the most promising compound was found to be **3a** with antiviral activity around 90 nM in a virus yield reduction assay. Unfortunately, the solubility rates of **3a** and **2** are equally low, which stands in strong contrast to analogs **2k** and **2o**. Accordingly, the latter were advanced to pharmacokinetic studies in the Sprague-Dawley rat model. Analog **2o** displays a 10-fold exposure (AUC/C_{max}) increase in this model relative to **2** and displays near dose proportionality in the range of 10 to 50 mg/kg. The Caco-2 permeability assessment demonstrated the high permeability of this class of molecule. This significant solubility increase might be a major determinant for the overall improvement in oral bioavailability. Compound **2o** was therefore identified as a second-generation lead for further development towards a novel measles therapeutic.

EXPERIMENTAL SECTION

GENERAL

Unless otherwise noted, all materials were obtained from commercial suppliers and used without purification. Dry organic solvents (DriSolv) were purchased from EMD Chemicals and packaged under nitrogen in Sure Seal bottles. Reactions were monitored using thin-layer chromatography on 250 μ m plates or using Agilent 1100 series LC/MS with UV detection at 254 nm and low resonance electrospray mode (ESI). Elemental analysis was done by Atlantic Microlab. Purification of title compounds was accomplished by liquid chromatography on a Biotage SP4 purification system with normal phase silica gel. ¹H NMR spectra were recorded on a Varian spectrometer (400 MHz) at ambient temperature. Chemical shifts are reported in ppm relative to CDCl₃ or CD₃OD and coupling constants (*J*) are reported in hertz (Hz). Solvents for NMR were deuteriochloroform (CDCl₃) (residual shifts: δ 7.26 for ¹H and δ 77.7 for ¹³C) and deuteriomethanol (CD₃OD) (residual shift: δ 3.31 for ¹H). The residual shifts were taken as internal references and reported in parts per million (ppm). Purities of all compounds were >95% determined by high performance liquid chromatography (HPLC) with UV detection at two wavelengths of 220 and 254 nm. Purities of key compounds were also confirmed by elemental analysis.

Typical Procedures for the Synthesis of 1-methyl-N-(4-(piperidin-1-ylsulfonyl)phenyl)-3-(trifluoromethyl)-1H-pyrazole-5-carboxamides (1a-c)—4-Amino-sulfonamide **7a-c** (1.0 mmol) in dichloromethane (5 ml) and pyridine (0.1 ml) was treated with 1-methyl-3-trifluoromethyl-5-pyrazolecarbonyl chloride (**8**) at rt. Reaction was monitored by LC-MS till no more starting material was seen, then the mixture was poured into saturated aqueous NaHCO₃ (10 ml), extracted with CH₂Cl₂ (3 \times 10ml). The CH₂Cl₂ extracts were collected and dried over anhydrous Na₂SO₄. Products were purified by chromatography.

N-(4-((2-((Methoxymethoxy)methyl)piperidin-1-yl)sulfonyl)phenyl)-1-methyl-3-(trifluoromethyl)-1H-pyrazole-5-carboxamide (1a)—¹H NMR (CDCl₃, 400MHz): δ 8.17 (s, 1H), 7.74 - 7.79 (m, 2H), 7.64 - 7.69 (m, 2H), 7.06 (s, 1H), 4.51 (s, 2H), 4.19 - 4.28 (m, 4H), 3.76-3.68 (m, 1H), 3.54 - 3.65 (m, 2H), 3.27 (s, 3H), 3.03-2.94 (m, 1H), 1.76-1.70 (m, 1H), 1.42 - 1.60 (m, 4H), 1.20 - 1.37 (m, 1H). Anal. calcd for C₂₁H₂₉F₃N₄O₅S: C, 49.79; H, 5.77; N, 11.06. Found: C, 49.07; H, 5.06; N, 11.31.

N-(4-((3-((Methoxymethoxy)methyl)piperidin-1-yl)sulfonyl)phenyl)-1-methyl-3-(trifluoromethyl)-1H-pyrazole-5-carboxamide (1b)—¹H NMR (CDCl₃, 400MHz): δ 8.09 (s, 1H), 7.69 - 7.78 (m, 4H), 7.03 (s, 1H), 4.56 (s, 2H), 4.25 (s, 3H), 3.78 (d, *J* = 11.7

Hz, 2H), 3.30 - 3.38 (m, 5H), 2.27 (td, $J=2.3, 11.9$ Hz, 2H), 1.72 - 1.83 (m, 2H), 1.50 (m, 1H), 1.29 - 1.42 (m, 2H); LC-MS (ESI) (LCT, 3 min) Rt 1.58 min; >95% purity at λ 254 and 210 nm, MS: m/z 491.5 [M+1].

***N*-4-((4-((Methoxymethoxy)methyl)piperidin-1-yl)sulfonyl)phenyl)-1-methyl-3-(trifluoromethyl)-1*H*-pyrazole-5-carboxamide (1c)**— ^1H NMR (CDCl_3 , 400MHz): δ 7.97 (s, 1H), 7.71 - 7.77 (m, 4H), 7.01 (s, 1H), 4.56 (s, 2H), 4.26 (s, 3H), 3.79 (d, $J=11.3$ Hz, 2H), 3.30 - 3.38 (m, 5H), 2.27 (td, $J=2.5, 11.8$ Hz, 2H), 1.79 (d, $J=10.6$ Hz, 2H), 1.45 - 1.56 (m, 1H), 1.35 (m, 2H). Anal. calcd for $\text{C}_{21}\text{H}_{29}\text{F}_3\text{N}_4\text{O}_5\text{S}$: C, 49.79; H, 5.77; N, 11.06. Found: C, 49.17; H, 5.09; N, 11.21.

Synthesis of *N*-4-((2-(hydroxymethyl)piperidin-1-yl)sulfonyl)phenyl)-1-methyl-3-(trifluoromethyl)-1*H*-pyrazole-5-carboxamide (2a)—A solution of (1-((4-nitrophenyl)sulfonyl)piperidin-2-yl)methanol **6a** (90 mg, 0.3 mmol) in MeOH (10 ml) was treated with H_2 (50 Psi) for 4 h in the presence of Pd/C (32 mg, 0.03 mmol). The Pd/C residue was removed by filtration, followed by evaporation of the solvent. The crude product was purified by chromatography (Hexane/EtOAc) to obtain amine product as white solid 70 mg (Y=86%).

4-Amino-sulfonamide (70 mg, 0.25 mmol) in dichloromethane (5 ml) and pyridine (0.1 ml) was treated with 1-methyl-3-trifluoromethyl-5-pyrazolecarbonyl chloride (**8**) at rt. Reaction was monitored by LC-MS till no more starting material was seen, then the mixture was poured into saturated aqueous NaHCO_3 (10 ml), extracted with CH_2Cl_2 ($3 \times 10\text{ml}$). The CH_2Cl_2 extracts were collected and dried over anhydrous Na_2SO_4 . Products were purified by chromatography (Hex/EtOAc) to obtain product **2a** as light yellow solid (81 mg, 73%). ^1H NMR (400MHz, CDCl_3) δ 1.23-1.62 (6H, m), 2.20 (1H, m), 3.08 (1H, t, $J=13.2$ Hz), 3.53-3.59 (1H, m), 3.77 (1H, d, $J=14.0\text{Hz}$), 3.84 (1H, t, $J=10.4\text{Hz}$), 4.00-4.06 (1H, m), 4.26 (3H, s), 7.11 (1H, s), 7.74-7.81 (4H, m), 8.48 (1H, s). Anal. calcd for $\text{C}_{18}\text{H}_{21}\text{F}_3\text{N}_4\text{O}_4\text{S}$: C, 48.43; H, 4.74; N, 12.55. Found: C, 48.33 ; H, 4.84 ; N, 12.23.

General Procedure for the Synthesis of Morpholinyl Analog (2b, 2n and 2o)—To a solution of aldehyde (1.0 mmol) in CH_2Cl_2 (10 ml) was added morpholine (1.3 eq, 1.3 mmol) and $\text{NaBH}(\text{OAc})_3$ (2.0 eq, 2.0 mmol) and the mixture was kept stirring at room temperature for 3h. NaHCO_3 (sat. aq) was added and the organic layer separated and washed with brine, dried over Na_2SO_4 , filtered and concentrated. The product was purified by column to give morpholinyl analog.

1-Methyl-*N*-4-((2-(morpholinomethyl)piperidin-1-yl)sulfonyl)phenyl)-3-(trifluoromethyl)-1*H*-pyrazole-5-carboxamide (2b)— ^1H NMR (CDCl_3 , 400MHz): δ 8.03 (s, 1H), 7.83 - 7.89 (m, 2H), 7.67 - 7.72 (m, 2H), 7.02 (s, 1H), 4.26 (s, 3H), 4.21 (br. s., 1H), 3.64 (m, 5H), 2.88 - 2.97 (m, 1H), 2.38 - 2.51 (m, 6H), 1.77 (m, 1H), 1.41 - 1.58 (m, 4H), 1.31(m, 1H). Anal. calcd for $\text{C}_{22}\text{H}_{28}\text{F}_3\text{N}_5\text{O}_4\text{S}$: C, 51.25; H, 5.47; N, 13.58. Found: C, 51.05; H, 5.45; N, 13.42.

***N*-4-((2-(Azidomethyl)piperidin-1-yl)sulfonyl)phenyl)-1-methyl-3-(trifluoromethyl)-1*H*-pyrazole-5-carboxamide (2c)**— ^1H NMR (CDCl_3 , 400MHz): δ 7.93 (s, 1H), 7.80 - 7.86 (m, 2H), 7.69 - 7.75 (m, 2H), 6.99 (s, 1H), 4.26 (s, 3H), 4.16 (m, 1H), 3.79 (d, $J=13.3$ Hz, 1H), 3.51 (dd, $J=7.2, 12.3$ Hz, 1H), 3.30 - 3.38 (m, 1H), 2.92 - 3.02 (m, 1H), 1.65 - 1.71 (m, 1H), 1.53 - 1.62 (m, 5H).

***N*-4-((2-(Aminomethyl)piperidin-1-yl)sulfonyl)phenyl)-1-methyl-3-(trifluoromethyl)-1*H*-pyrazole-5-carboxamide (2d)**— ^1H NMR (CDCl_3 , 400MHz): δ

8.27 (s, 1H), 7.77 - 7.83 (m, 2H), 7.68 - 7.75 (m, 2H), 7.03 (s, 1H), 4.25 (s, 3H), 3.87 - 3.96 (m, 1H), 3.77 (d, $J = 11.0$ Hz, 1H), 2.92 - 3.06 (m, 2H), 2.64 (dd, $J = 5.7, 13.5$ Hz, 1H), 1.28 - 1.60 (m, 6H). LC-MS (ESI) (LCT, 3 min) Rt 0.54 min; >95% purity at λ 254 and 210 nm, MS: m/z 446.0 [M+1].

***N*-(4-((2-(Acetamidomethyl)piperidin-1-yl)sulfonyl)phenyl)-1-methyl-3-(trifluoromethyl)-1*H*-pyrazole-5-carboxamide (2e)**— ^1H NMR (CDCl_3 , 400MHz): δ 9.31 (s, 1H), 7.83 - 7.90 (m, 2H), 7.76 - 7.82 (m, 2H), 7.22 (s, 1H), 6.08 (t, $J = 5.5$ Hz, 1H), 4.26 (s, 3H), 4.03 - 4.13 (m, 1H), 3.67 - 3.77 (m, 1H), 3.56 (ddd, $J = 5.3, 10.9, 14.0$ Hz, 1H), 3.20 - 3.28 (m, 1H), 3.02 - 3.11 (m, 1H), 2.0 (m, 3H), 1.38 - 1.53 (m, 4H), 1.20 - 1.34 (m, 1H). Anal. calcd for $\text{C}_{20}\text{H}_{25}\text{F}_3\text{N}_4\text{O}_4\text{S}$: C, 49.28; H, 4.96; N, 14.37. Found: C, 49.02; H, 4.98; N, 14.08.

(*E*)-Ethyl 3-(1-((4-(1-methyl-3-(trifluoromethyl)-1*H*-pyrazole-5-carboxamido)phenyl)-sulfonyl)piperidin-2-yl)acrylate (2g)— ^1H NMR (CDCl_3 , 400MHz): δ 8.19 (s, 1H), 7.69 - 7.78 (m, 4H), 7.03 (s, 1H), 6.75 (dd, $J = 4.0, 16.0$ Hz, 1H), 5.89 (dd, $J = 2.0, 16.0$ Hz, 1H), 4.69 (br. s., 1H), 4.25 (s, 3H), 4.15 (q, $J = 7.0$ Hz, 2H), 3.67 (d, $J = 12.9$ Hz, 1H), 2.95 - 3.05 (m, 1H), 1.63 - 1.78 (m, 2 H), 1.56 (d, $J = 11.0$ Hz, 7 H), 1.32 - 1.47 (m, 7 H), 1.25 (t, $J = 8.0$ Hz, 3H). Anal. calcd for $\text{C}_{22}\text{H}_{25}\text{F}_3\text{N}_4\text{O}_5\text{S}$: C, 51.36; H, 4.90; N, 10.89. Found: C, 51.42; H, 4.90; N, 10.79.

(*E*)-*N*-(4-((2-(3-Hydroxyprop-1-en-1-yl)piperidin-1-yl)sulfonyl)phenyl)-1-methyl-3-(trifluoromethyl)-1*H*-pyrazole-5-carboxamide (2h)— ^1H NMR (CDCl_3 , 400MHz): δ 8.32 (s, 1H), 7.63 - 7.77 (m, 4H), 7.05 - 7.10 (m, 1H), 5.63 - 5.72 (m, 1H), 5.52 - 5.61 (m, 1H), 4.54 (br. s., 1H), 4.24 (s, 3H), 3.95 - 4.08 (m, 2H), 3.64 (d, $J = 12.5$ Hz, 1H), 3.47 (d, $J = 5.1$ Hz, 1H), 2.91 - 3.02 (m, 1H), 1.81 (t, $J = 5.9$ Hz, 1H), 1.34 - 1.74 (m, 6H). Anal. calcd for $\text{C}_{20}\text{H}_{23}\text{F}_3\text{N}_4\text{O}_4\text{S}$: C, 50.84; H, 4.91; N, 11.86. Found: C, 50.57; H, 4.98; N, 11.63.

Ethyl 3-(1-((4-(1-methyl-3-(trifluoromethyl)-1*H*-pyrazole-5-carboxamido)phenyl)-sulfonyl)piperidin-2-yl)propanoate (2i)— ^1H NMR (CDCl_3 , 400MHz): δ 8.34 (s, 1H), 7.66 - 7.83 (m, 4H), 7.07 (s, 1H), 4.25 (s, 3H), 4.02 (s, 1H), 3.73 (d, $J = 14.5$ Hz, 1H), 3.63 (m, 2H), 2.93 - 3.05 (m, 1H), 2.16 (s, 3H), 1.59 - 1.81 (m, 2H), 1.28 - 1.59 (m, 6H). LC-MS (ESI) (LCT, 3 min) Rt 2.11 min; >95% purity at λ 254 and 210 nm, MS: m/z 517.1 [M+1].

***N*-(4-((2-(3-Hydroxypropyl)piperidin-1-yl)sulfonyl)phenyl)-1-methyl-3-(trifluoromethyl)-1*H*-pyrazole-5-carboxamide (2j)**— ^1H NMR (CHLOROFORM-d , 400MHz): δ 8.26 (s, 1H), 7.67 - 7.79 (m, 4H), 7.06 (s, 1H), 4.25 (s, 3H), 4.11 (q, $J = 7.0$ Hz, 2H), 3.99 - 4.07 (m, 1H), 3.74 (d, $J = 14.5$ Hz, 1H), 2.96 - 3.07 (m, 1H), 2.36 (t, $J = 7.4$ Hz, 2H), 2.00 - 2.13 (m, 1H), 1.60 - 1.72 (m, 1H), 1.30 - 1.55 (m, 5H), 1.24 (t, $J = 7.2$ Hz, 3H), 1.01 - 1.17 (m, 1H). Anal. calcd for $\text{C}_{20}\text{H}_{25}\text{F}_3\text{N}_4\text{O}_4\text{S}$: C, 50.62; H, 5.31; N, 11.81. Found: C, 50.35; H, 5.28; N, 11.62.

***N*-(4-((2-(2-Hydroxyethyl)piperidin-1-yl)sulfonyl)phenyl)-1-methyl-3-(trifluoromethyl)-1*H*-pyrazole-5-carboxamide (2k)**— ^1H NMR (CDCl_3 , 400MHz): δ 8.00 (s, 1H), 7.86 (d, $J = 8.6$ Hz, 2H), 7.75 (d, $J = 8.6$ Hz, 2H), 6.99 (s, 1H), 4.26 (s, 3H), 4.17 - 4.25 (m, 1H), 3.90 (d, $J = 14.1$ Hz, 1H), 3.74 - 3.83 (m, 1H), 3.67 (d, $J = 5.1$ Hz, 1H), 2.97 - 3.06 (m, 1H), 2.84 (dd, $J = 4.9, 8.4$ Hz, 1H), 1.93 - 2.02 (m, 1H), 1.40 - 1.54 (m, 5H), 1.32-1.40 (M, 1H). Anal. calcd for $\text{C}_{19}\text{H}_{23}\text{F}_3\text{N}_4\text{O}_4\text{S}$: C, 49.56; H, 5.03; N, 12.17. Found: C, 49.36; H, 5.08; N, 11.98.

(R)-N-(4-((2-(2-Hydroxyethyl)piperidin-1-yl)sulfonyl)phenyl)-1-methyl-3-(trifluoromethyl)-1H-pyrazole-5-carboxamide (2l)—¹H NMR (CDCl₃, 400MHz): δ 8.34 (s, 1H), 7.84 (d, *J* = 8.4 Hz, 2H), 7.78 (d, *J* = 8.4 Hz, 2H), 7.07 (s, 1H), 4.27 (s, 3H), 4.22 - 4.19 (m, 1H), 3.91 (d, *J* = 14.4 Hz, 1H), 3.80 (t, *J* = 11.2 Hz, 1H), 3.67 (br, 1H), 3.06 - 2.04 (m, 2H), 2.03-1.95 (m, 1H), 1.57 - 1.41 (m, 4H), 1.28-1.21 (m, 2H). LC-MS (ESI) (LCT, 3 min) Rt 1.09 min; >95% purity at λ 254 and 210 nm, MS: *m/z* 461.2 [M+1].

(S)-N-(4-((2-(2-Hydroxyethyl)piperidin-1-yl)sulfonyl)phenyl)-1-methyl-3-(trifluoromethyl)-1H-pyrazole-5-carboxamide (2m)—¹H NMR (CDCl₃, 400MHz): δ 8.12 (m, 1H), 7.86 (d, *J* = 8.6 Hz, 2H), 7.75 (d, *J* = 8.6 Hz, 2H), 7.03 (s, 1H), 4.28 (s, 3H), 4.20 - 4.23 (m, 1H), 3.91 (d, *J* = 14.1 Hz, 1H), 3.81 (t, *J* = 11.6 Hz, 1H), 3.68 (m, 1H), 3.03 (t, *J* = 12.8 Hz, 1H), 2.88 (m, 1H), 2.05 - 1.96 (m, 1H), 1.58-1.26 (m, 5H), 1.13-1.08 (m, 1H). LC-MS (ESI) (LCT, 3 min) Rt 1.09 min; >95% purity at λ 254 and 210 nm, MS: *m/z* 461.2 [M+1]. Anal. calcd for C₁₉H₂₃F₃N₄O₄S: C, 49.56; H, 5.03; N, 12.17. Found: C, 49.50; H, 5.05; N, 11.95.

(S)-1-methyl-N-(4-((2-(2-morpholinoethyl)piperidin-1-yl)sulfonyl)phenyl)-3-(trifluoromethyl)-1H-pyrazole-5-carboxamide (2o)—¹H NMR (CDCl₃, 400MHz): δ 8.18 (s, 1H), 7.74 - 7.80 (m, 2H), 7.65 - 7.72 (m, 2H), 7.05 (s, 1H), 4.25 (s, 3H), 4.04 - 4.11 (m, 1H), 3.76 (dd, *J* = 4.1, 14.3 Hz, 1H), 3.67 (t, *J* = 4.5 Hz, 1H), 2.97 - 3.08 (m, 1H), 2.23 - 2.45 (m, 6H), 1.78 - 1.90 (m, 1H), 1.55 - 1.66 (m, 1H), 1.30 - 1.53 (m, 5H). LC-MS (ESI) (LCT, 3 min) Rt 0.57 min; >95% purity at λ 254 and 210 nm, MS: *m/z* 530.2 [M+1]. Anal. calcd for C₂₃H₃₀F₃N₅O₄S.H₂O: C, 50.45; H, 5.89; N, 12.79. Found: C, 50.98; H, 5.72; N, 12.74.

Ethyl 2-((1-((4-(1-methyl-3-(trifluoromethyl)-1H-pyrazole-5-carboxamido)phenyl)sulfonyl)piperidin-2-yl)methoxy)acetate (2p)—¹H NMR (CDCl₃, 400MHz): δ 8.14 (s, 1H), 7.77 - 7.83 (m, 2H), 7.65 - 7.70 (m, 2H), 7.02 - 7.06 (m, 1H), 4.25 (s, 3H), 4.14 - 4.23 (m, 3H), 3.99 (d, *J* = 3.1 Hz, 2H), 3.73 (d, *J* = 14.1 Hz, 1H), 3.60 - 3.67 (m, 2H), 2.96 - 3.06 (m, 1H), 1.77 (d, *J* = 12.9 Hz, 1H), 1.37 - 1.56 (m, 3H), 1.26 (t, *J* = 8.0 Hz, 3H). LC-MS (ESI) (LCT, 3 min) Rt 1.71 min; >95% purity at λ 254 and 210 nm, MS: *m/z* 533.2 [M+1].

N-(4-((2-(2-hydroxyethoxy)methyl)piperidin-1-yl)sulfonyl)phenyl)-1-methyl-3-(trifluoromethyl)-1H-pyrazole-5-carboxamide (2q, JMN6-093)—¹H NMR (CDCl₃, 400MHz): δ 8.73 (s, 1H), 7.70 - 7.83 (m, 4H), 7.11 (s, 1H), 4.30 - 4.39 (m, 1H), 4.25 (s, 3H), 3.72 (t, *J* = 9.4 Hz, 2H), 3.58 - 3.68 (m, 2H), 3.45 - 3.54 (m, 2H), 3.40 (d, *J* = 10.6 Hz, 1H), 3.25 (br. s., 1H), 2.98 (td, *J* = 2.5, 13.2 Hz, 1H), 1.63 - 1.74 (m, 2H), 1.35 - 1.63 (m, 3H). Anal. calcd for C₂₀H₂₅F₃N₄O₅S: C, 48.97; H, 5.14; N, 11.42. Found: C, 48.94; H, 5.08; N, 11.26.

1-Methyl-N-(4-(phenylsulfonyl)phenyl)-3-(trifluoromethyl)-1H-pyrazole-5-carboxamide (3a)—¹H NMR (CDCl₃, 400MHz): δ 8.10 (s, 1H), 7.85 - 7.93 (m, 4H), 7.69 - 7.75 (m, 2H), 7.53 - 7.59 (m, 1H), 7.46 - 7.53 (m, 2H), 7.03 (s, 1H), 4.22 (s, 3H). Anal. calcd for C₁₈H₁₄F₃N₃O₃S: C, 52.81; H, 3.45; N, 10.26. Found: C, 52.31; H, 3.41; N, 9.95.

N-(4-((2-methoxyphenyl)sulfonyl)phenyl)-1-methyl-3-(trifluoromethyl)-1H-pyrazole-5-carboxamide (3b)—¹H NMR (CDCl₃, 400MHz): δ 8.11 (dd, *J* = 1.8, 8.0 Hz, 1H), 8.04 (s, 1H), 7.90 - 7.95 (m, 2H), 7.66 - 7.71 (m, 2H), 7.51 - 7.57 (m, 1 H), 7.07 - 7.13 (m, 1 H), 7.02 (s, 1 H), 6.87 - 6.91 (m, 1 H), 4.24 (s, 3 H), 3.76 (s, 3H). LC-MS (ESI) (LCT, 3 min) Rt 1.11 min; >95% purity at λ 254 and 210 nm, MS: *m/z* 440.0 [M+1].

Synthesis of *N*-(4-((2-Hydroxyphenyl)sulfonyl)phenyl)-1-methyl-3-(trifluoromethyl)-1*H*-pyrazole-5-carboxamide (3c)—To a solution of **3b** (110.0 mg, 0.250 mmol) in CH₂Cl₂ (6.0 mL), was added BBr₃ (1.0 mL, 1.0 mmol) and the mixture stirred for an overnight. The reaction was cooled to 0 °C and NaHCO₃ solution (3.0 mL) slowly added. The reaction was allowed to warm to RT and CH₂Cl₂ (9.0 mL) and MeOH (1.0 mL) added. The organic layer was separated and washed with NaHCO₃, brine, dried over Na₂SO₄, filtered and concentrated. The product was purified by column (CH₂Cl₂/MeOH) and dried under vacuum to give 106.0 mg of a white solid in 96% yield. ¹H NMR (CDCl₃, 400MHz): δ 7.86 - 7.92 (m, 2 H), 7.77 - 7.82 (m, 2 H), 7.65 (dd, *J* = 1.6, 8.2 Hz, 1 H), 7.37 - 7.43 (m, 1H), 7.11 (s, 1H), 6.90 - 6.96 (m, 2H), 4.20 (s, 3H). Anal. calcd for C₁₈H₁₄F₃N₃O₄S: C, 50.82; H, 3.32; N, 9.88. Found: C, 50.67; H, 3.29; N, 9.61.

Synthesis of 2-((4-(1-Methyl-3-(trifluoromethyl)-1*H*-pyrazole-5-carboxamido)phenyl)sulfonyl)phenylacetate (3d)—To a solution of **3c** (52.0 mg, 0.122 mmol) in dimethylformamide (1.0 mL) was added K₂CO₃ (33.8 mg, 0.244 mmol) and acetic anhydride (0.023 mL, 0.244 mmol) and the mixture allowed to stir for an overnight. DMF was removed under vacuum and the residue purified by column (hexanes/ethylacetate) to give 43.4 mg of **3d** as a white solid in 76% yield. ¹H NMR (CDCl₃, 400 MHz) δ 8.14 (dd, *J* = 1.76, 8.02 Hz, 1H), 7.87 - 7.93 (m, 3H), 7.70 - 7.76 (m, 2H), 7.58 - 7.63 (m, 1H), 7.41 (dt, *J* = 1.17, 7.83 Hz, 1H), 7.14 (dd, *J* = 0.98, 8.02 Hz, 1H), 6.96 (s, 1H), 4.24 (s, 3H), 2.32 (s, 3H). Anal. calcd for C₂₀H₁₆F₃N₃O₅S: C, 51.39; H, 3.45; N, 8.99. Found: C, 51.31; H, 3.32; N, 8.80.

1-Methyl-3-(trifluoromethyl)-*N*-(4-((2-vinylphenyl)sulfonyl)phenyl)-1*H*-pyrazole-5-carboxamide (3e)—¹H NMR (CDCl₃, 400 MHz) δ 8.12 - 8.17 (m, 1H), 8.08 (s, 1H), 7.76 - 7.83 (m, 2H), 7.65 - 7.71 (m, 2H), 7.51 - 7.59 (m, 2H), 7.41 - 7.50 (m, 2H), 7.02 (s, 1H), 5.52 (dd, *J* = 1.17, 17.22 Hz, 1H), 5.33 (dd, *J* = 0.78, 10.96 Hz, 1H), 4.22 (s, 3H). Anal. calcd for C₂₀H₁₆F₃N₃O₃S: C, 55.17; H, 3.70; N, 9.65. Found: C, 54.99; H, 3.60; N, 9.64.

***N*-(4-((2-(Hydroxymethyl)phenyl)sulfonyl)phenyl)-1-methyl-3-(trifluoromethyl)-1*H*-pyrazole-5-carboxamide (3f)**—¹H NMR (CDCl₃, 400 MHz) δ 8.10 (dd, *J* = 1.17, 7.83 Hz, 1H), 8.00 (s, 1H), 7.84 - 7.90 (m, 2H), 7.71 - 7.77 (m, 2H), 7.59 - 7.65 (m, 1H), 7.48 - 7.57 (m, 2H), 6.98 (s, 1H), 4.73 (d, *J* = 6.26 Hz, 2H), 4.23 (s, 3H). Anal. calcd for C₁₉H₁₆F₃N₃O₄S: C, 51.93; H, 3.67; N, 9.56. Found: C, 52.01; H, 3.53; N, 9.40.

1-Methyl-*N*-(4-((2-(morpholinomethyl)phenyl)sulfonyl)phenyl)-3-(trifluoromethyl)-1*H*-pyrazole-5-carboxamide (3g)—¹H NMR (CDCl₃, 400MHz): δ 8.16 (dd, *J* = 1.2, 7.8 Hz, 1 H), 7.99 (s, 1H), 7.83 - 7.89 (m, 2H), 7.68 - 7.74 (m, 3H), 7.54 - 7.60 (m, 1H), 7.42 - 7.48 (m, 1H), 7.01 (s, 1H), 4.24 (s, 3H), 3.77 (s, 2H), 3.50 - 3.57 (m, 4H), 2.27 (m, 4H). Anal. calcd for C₂₃H₂₃F₃N₄O₄S: C, 54.32; H, 4.56; N, 11.02. Found: C, 54.36; H, 4.42; N, 10.85.

BIOLOGY

Antiviral assays and toxicity measurements were performed as described previously.²²

Supplementary Material

Refer to Web version on PubMed Central for supplementary material.

Acknowledgments

This work was supported, in part, by Public Health Service Grants AI071002 and AI085328 (to R. K. P.) from the NIH/NIAID and by Public Health Service Grant HG003918-02 (to J.P.S.) from the NIH. We gratefully acknowledge significant funding support from The Emory Institute for Drug Discovery. We are also grateful to Deborah Culver for solubility testing.

ABBREVIATION USED

MeV	measles virus
RNA	ribonucleic acid
RdRp	RNA dependent RNA polymerase
HTS	high-throughput screening
HPIV	human parainfluenza virus
RSV	respiratory syncytial virus
EC₅₀	50% effective concentration
CC₅₀	50% cytotoxicity concentration
MOM	methoxymethyl
TBSCI	<i>t</i> -butyldimethylsilyl chloride
DIBALH	diisobutylaluminium hydride
MCPBA	meta-chloroperoxybenzoic acid
PK	pharmacokinetic

REFERENCES

- (1). Centers for Disease Control and Prevention. Update: measles-United States, January-July 2008. *MMWR Morb. Mortal.* 2008; 57:893–896. *Wkly. Rep.*
- (2). Kremer JR, Muller CP. Measles in Europe—there is room for improvement. *Lancet.* 2009; 373:356–358. [PubMed: 19131098]
- (3). [last accessed 12/16/11] http://www.oregonlive.com/opinion/index.ssf/2011/01/vaccines_haltng_an_epidemic_o.html; <http://www.pbs.org/wgbh/pages/frontline/vaccines/view/>
- (4). http://www.who.int/csr/don/2011_04_21/en/
- (5). Chakrabarti S, Collingham KE, Holder K, Fegan CD, Osman H, Milligan DW. Pre-emptive oral ribavirin therapy of paramyxovirus infections after haematopoietic stem cell transplantation: a pilot study. *Bone Marrow Transplant.* 2001; 21:759–763. [PubMed: 11781627]
- (6). Shigeta S, Mori S, Baba M, Ito M, Honzumi K, Nakamura K, Oshitani H, Numazaki Y, Matsuda A, T. Obara T, Shuto S, De Clercq E. Antiviral activities of ribavirin, 5-ethynyl-1--D-ribofuranosylimidazole-4-carboxamide, and 6-(*R*)-6-*C*-methylneplanocin A against several ortho- and paramyxoviruses. *Antimicrob. Agents Chemother.* 1992; 36:435–439. [PubMed: 1605607]
- (7). Plemper RK, Snyder JP. Measles control - can measles virus inhibitors. *Current Opinion in Investigational Drugs.* 2009; 10:811–820. (BioMed Central). [PubMed: 19649926]
- (8). White LK, Yoon J-J, Lee JK, Sun A, Du Y, Fu H, Snyder JP, Plemper RK. Non nucleoside Inhibitor of Measles Virus RNA Dependent RNA Polymerase Complex Activity. *Antimicrob. Agents Chemother.* 2007; 51:2293–2303. [PubMed: 17470652]
- (9). Yoon J, Krumm SA, Ndungu JM, Hoffman V, Bankamp B, Rota PA, Sun A, Snyder JP, Plemper RK. Target analysis of the experimental measles therapeutic AS-136A *Antimicrob. Agents and Chemother.* 2009; 53:3860–3870.

- (10). Sun A, Chandrakumar N, Yoon J-J, Plemper RK, Snyder JP. Non nucleoside inhibitors of the measles virus RNA-dependent RNA polymerase activity: Synthesis and in vitro evaluation. *Bioorg. Med. Chem. Lett.* 2007; 17:5199–5203. [PubMed: 17643302]
- (11). Sun A, Yoon JJ, Yin Y, Prussia A, Yang Y, Min, J, Plemper RK, Snyder JP. Potent non-nucleoside inhibitors of the measles virus RNA-dependent RNA polymerase complex. *J. Med. Chem.* 2008; 51:3731–3741. [PubMed: 18529043]
- (12). Lahm GP, Selby TP, Freudenberger JH, Stevenson TM, Myers BJ, Seburyamo G, Smith BK, Flexner L, Clark CE, Cordova D. Insecticidal anthranilic diamides: A new class of potent ryanodine receptor activators. *Bioorg. Med. Chem. Lett.* 2005; 15:4898–4906. [PubMed: 16165355]
- (13). See supporting information for a detailed synthesis of **2a** and related compounds.
- (14). Tanaka M, Nakamura M, Ikeda T, Ikeda K, Ando H, Shibutani Y, Yajima S, Kimura K. *J. Org. Chem.* 2001; 66:7008–7012. [PubMed: 11597221]
- (15). Paulissen R, Reimlinger H, Hayez E, Hubert AJ, Teyssié P. Transition metal catalysed reaction of diazocompounds - II insertion in the hydroxylic bond. *Tetrahedron Lett.* 1973:2233–2236.
- (16). Moody CJ, Miller DJ. Synthetic applications of the O-H insertion reactions of carbenes and carbenoids derived from diazocarbonyl and related diazo compounds. *Tetrahedron.* 1995; 51:10811–10843.
- (17). McGeary RP. Facile and chemoselective reduction of carboxylic acids to alcohols using BOP reagent and sodium borohydride. *Tetrahedron Lett.* 1998; 39:3319.
- (18). Szadkowska A, Makal A, Wozniak K, Kadyrov R, Grela K. *Organometallics.* 2009; 28:2693–2700.
- (19). Sun H, Pang KS. Permeability, Transport, and Metabolism of Solutes in Caco-2 Cell Monolayers: A Theoretical Study. *Drug Metabolism and Disposition.* 2008; 36:102–123. [PubMed: 17932224]
- (20). Sarkadi B, Homolya L, Szakacs G, Varadi A. Human Multidrug Resistance ABCB and ABCG Transporters: Participation in a Chemoimmunity Defense System. *Physiol Rev.* 2006; 86:1179–1236. [PubMed: 17015488]
- (21). Krumm SA, Ndungu JM, Dochow M, Yoon J-J, Sun A, Natchus M, Snyder JP, Plemper RK. Host-Directed Small-Molecule Inhibitors of Myxovirus RNA-dependent RNA-polymerases. *PLoS ONE.* 10.1371/journal.pone.0020069.
- (22). Sun A, Ndungu JM, Krumm SA, Yoon Jeong-J, Thepchatri P, Natchus M, Plemper RK, Snyder JP. Host-directed Inhibitors of Myxoviruses: Synthesis and in vitro Biochemical Evaluation. *ACS Med. Chem. Lett.* 2011; 2:798–803. [PubMed: 22328961]

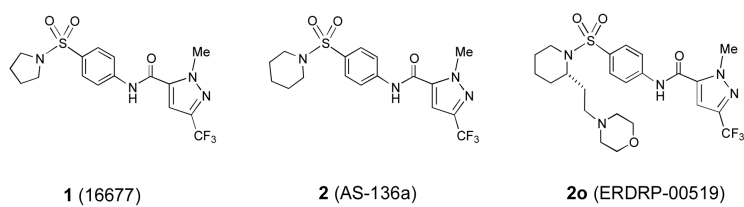


Figure 1.
Structures of hit and lead compounds.

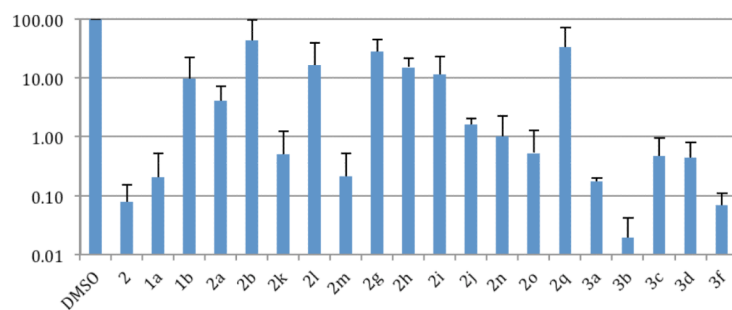


Figure 2. Evaluation of compounds **2** and analogs against MV-Alaska. All compounds were tested at 1.0 μ M. Compounds comparable in activity to **2** were further examined at a range of concentrations to generate dose-response curves.

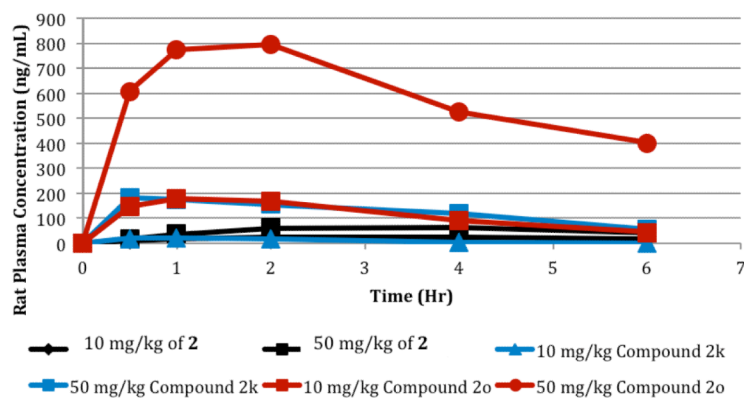


Figure 3. Time course of rat plasma concentration following p.o. dosing by oral gavage. Preliminary pharmacokinetic (PK) studies in the Sprague-Dawley rat compared **2** with compounds **2k** and **2o** following p.o. dosing by oral gavage at 10 mg/kg and 50 mg/kg in a PEG200/0.5% methylcellulose (10/90) vehicle (n=4/group)

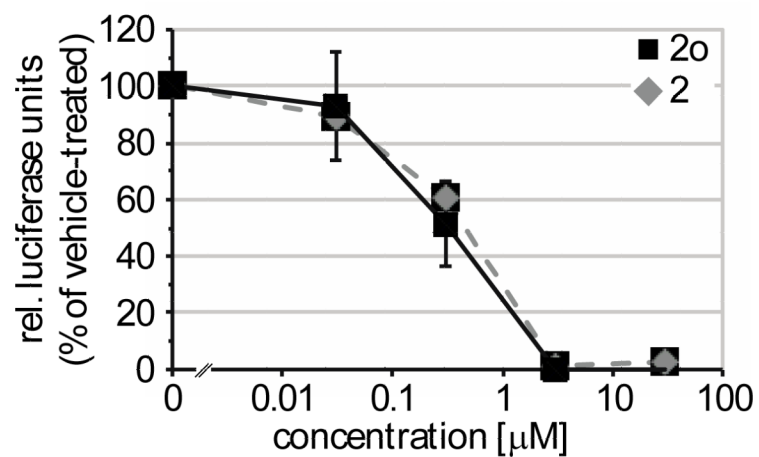
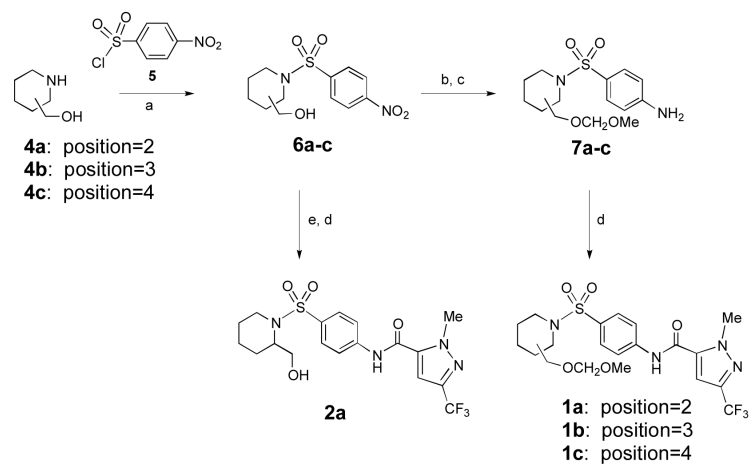
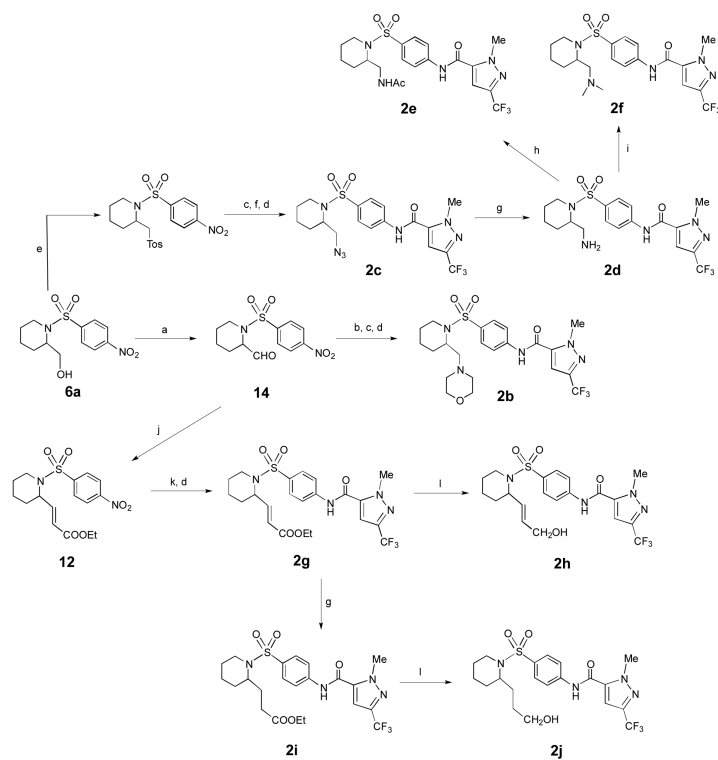


Figure 4. Compounds **2o** and **2** inhibit viral RdRp activity with equal potency. Values are expressed relative to vehicle-treated samples and represent averages of three experiments \pm SD.

**Scheme 1.**

Exploring the optimal substitution position on the piperidine ring^a

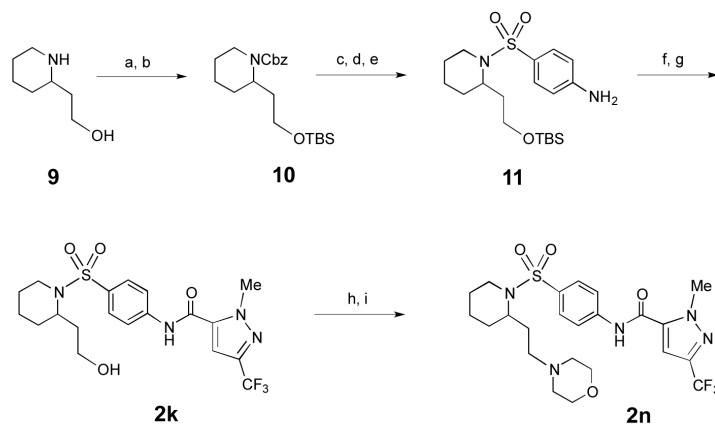
^aReagents and conditions: (a) Na₂CO₃, acetone; (b) MOMCl, *i*-Pr₂NEt, CH₂Cl₂; (c) SnCl₂·2H₂O, EtOAc; (d) **8**, Pyridine, CH₂Cl₂; (e) H₂ (50 psi), Pd-C, MeOH.



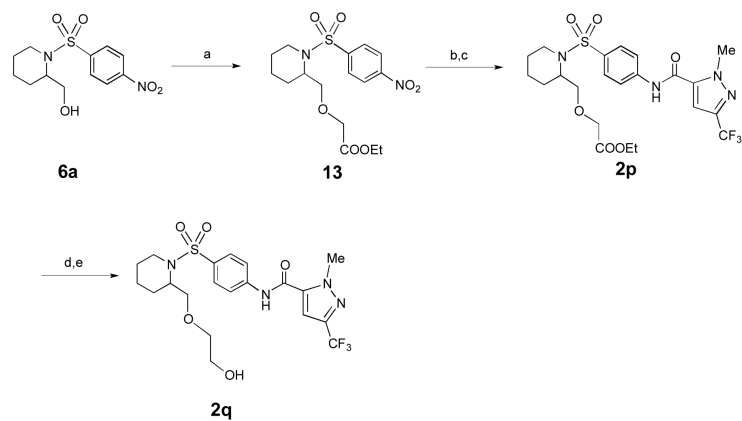
Scheme 2.

Synthesis of three-carbon substituents at the piperidine C-2 position^a

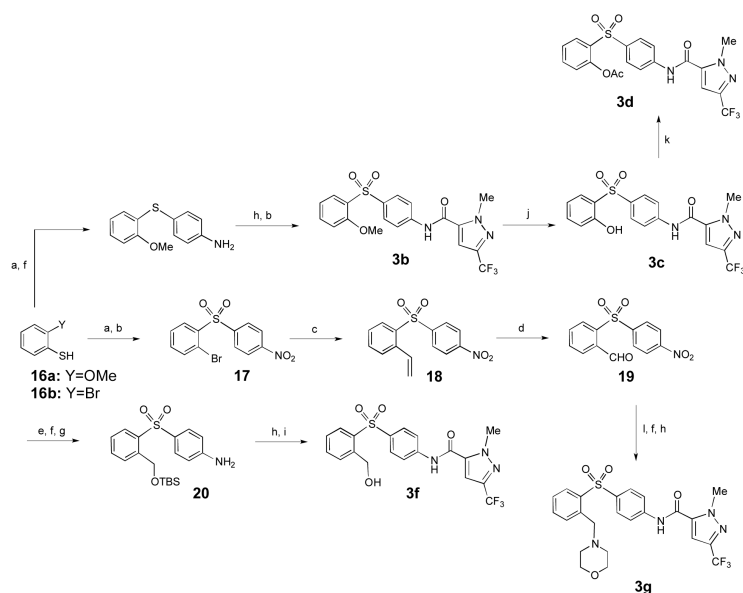
^aReagents and conditions: (a) PCC, CH₂Cl₂; (b) morpholine, NaBH(OAc)₃, CH₂Cl₂; (c) SnCl₂·2H₂O, CH₂Cl₂/MeOH; (d) **8**, *i*-Pr₂NEt, CH₂Cl₂; (e) 4-Toluenesulfonyl chloride, CH₂Cl₂; (f) NaN₃, DMF, 120 °C; (g) H₂, Pd/C, MeOH; (h) AcCl, *i*-Pr₂NEt, CH₂Cl₂; (i) CH₃I, K₂CO₃, DMF; (j) *t*-BuOK, Et₂P(O)CH₂COOEt, THF/CH₂Cl₂; (k) SnCl₂·2H₂O, EtOAc; (l) DIBAL-H, THF;

**Scheme 3.**Introduction of a two-carbon tether at the piperidine C-2 position^a

^aReagents and conditions: (a) Na₂CO₃, BzOCOCl, H₂O/acetone; (b) TBSCl, imidazole, DMF; (c) H₂, Pd/C, ethanol; (d) **5**, *i*-Pr₂NEt, CH₂Cl₂; (e) H₂, Pd/C, ethanol, 40 psi; (f) **8**, *i*-Pr₂NEt, CH₂Cl₂; (g) TBAF, THF; (h) (COCl)₂, DMSO, CH₂Cl₂; (i) morpholine, NaBH(OAc)₃, CH₂Cl₂.

**Scheme 4.**Synthesis of O-alkylated analogs^a

^aReagents and conditions: (a) ethyl diazoacetate, Rh₂OAc₄, CH₂Cl₂; (b) H₂, Pd/C, MeOH; (c) **8**, *i*-Pr₂NEt, CH₂Cl₂; (d) NaOH, THF/H₂O; (e) BOP, *i*-Pr₂NEt, THF, NaBH₄.

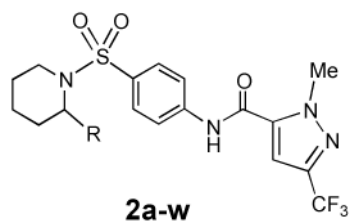


Scheme 5.


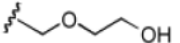
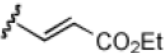
Synthesis of the phenyl series^a

^aReagents and conditions: (a) 1-fluoro-4-nitrobenzene, Na₂CO₃, EtOH, 80°C; (b) *m*-CPBA, CH₂Cl₂; (c) tributyl(vinyl)tin, Pd(PPh₃)₄, THF, 80°C; (d) OsO₄, NaIO₄, THF/H₂O; (e) DIBAL-H, THF; (f) SnCl₂·2H₂O, CH₂Cl₂/MeOH; (g) TBSCl, imidazole, DMF; (h) **8**, *i*-Pr₂NEt, CH₂Cl₂; (i) TBAF, THF; (j) BBr₃, CH₂Cl₂; (k) CH₃COCl, THF; (l) morpholine, NaBH(OAc)₃, CH₂Cl₂.

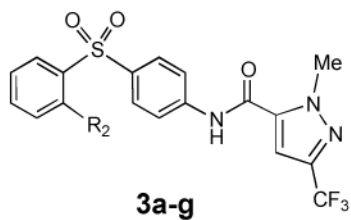
Table 1

MeV antiviral action (CPE) of the piperidine series of analogs, (EC₅₀).

Comp.	R	EC ₅₀ (μM) ^a (MV-Alaska) (CPE inhib.)	Comp.	R	EC ₅₀ (μM) ^a (MV-Alaska) (CPE inhib.)
2	-H	2.0	2h		3.7
1a		1.5	2i		6.7
1b		3.8	2j		2.7
1c		16.0	2k		2.7
2a		2.8	2l		8.3
2b		9.3	2m		3.1
2c		1.5	2n		4.6
2d		55.0	2o		2.5
2e		14.0	2p		25.0

Comp.	R	EC ₅₀ (μM) ^a (MV-Alaska) (CPE inhib.)	Comp.	R	EC ₅₀ (μM) ^a (MV-Alaska) (CPE inhib.)
2f		>150.0	2q		8.3
2g		6.8			

^a values represent averages of four experiments; highest concentration assessed 150 μM

Table 2MeV antiviral action (CPE) of the phenyl and acyclic series of analogs, (EC_{50}).

Comp.	R ²	EC ₅₀ (μM) ^a (MV-Alaska) (CPE inhib.)	Comp.	R ₂	EC ₅₀ (μM) ^a (MV-Alaska) (CPE inhib.)
3a	-H	2.8	3e		> 50.0
3b	-OMe	3.1	3f		3.5
3c	-OH	4.5	3g		>75.0
3d	-OAc	4.5			

^a values represent averages of four experiments; highest concentration assessed 75 μM

Table 3Aqueous solubility, virus yields (EC₅₀) and toxicity (CC₅₀) for selected compounds.

Comp.	Solubility ($\mu\text{g/ml}$) Test ^a	EC ₅₀ (μM) (MV-Alaska)		CC ₅₀ (μM) (MTT cytotox) ^d
		CPE inhibit. ^b	virus titer reduction ^c	
2	<15	2.0	0.014	>75
2a	61	2.8	0.85	>75
2k	62	2.7	0.1	>75
2n	55	4.6	nd	>75
2o	60	2.5	0.06	>75
3a	22	2.8	0.09	>75
3b	<15	3.1	nd	>75
3c	67	4.5	nd	75
3f	46	3.5	nd	>75

^a solubility data generated through Nephelometer using standard procedure.

^b Values represent averages of four experiments; highest concentration assessed 75 μM , lowest concentration assessed 2.0 μM .

^c Determined only when CPE inhibition-based EC50 concentration < 3.0 μM .

^d Values represent averages of at least three experiments; highest concentration assessed 75 μM .

Table 4PK Profile for Compounds **2**, **2k** and **2o**

Comp.	oral dose (mg/kg) ^a	T _{max} (hr)	C _{max} (ng/mL) ^b	T _{1/2} (hr) ^b	AUC (0-t) (hr*ng/mL) ^b	AUC (0-∞) (hr*ng/mL) ^b
2	10	2.5	26.9	12.7	132	513
2	50	2.7	72.2	3.7	308	483
2k	10	1	19.8	0.8	56.3	56.8
2k	50	0.5	184	2.7	754	973
2o	10	1.1	195	2.2	683	818
2o	50	1.5	823	6.5	3521	7860

^aStudy in Sprague-Dawley rat dosed at 10 mg/kg and 50 mg/kg as a suspension in PEG200/0.5% methylcellulose (10/90) formulation, respectively. n = 4 animals per study.

^bEstimation of PK parameters by non-compartmental analysis of these data, which was accomplished using standard PK software (WinNonlin 5.3, Pharsight®).